

Asymptotic regime for hadron-hadron diffractive collisions at ultrahigh energies

V.V. Anisovich

National Research Centre "Kurchatov Institute", Petersburg Nuclear Physics Institute, Gatchina 188300, Russia

V.A. Nikonov

*National Research Centre "Kurchatov Institute", Petersburg Nuclear Physics Institute, Gatchina 188300, Russia and
Helmholtz-Institut für Strahlen- und Kernphysik, Universität Bonn, 53115 Bonn, Germany*

J. Nyiri

Institute for Particle and Nuclear Physics, Wigner RCP, Budapest 1121, Hungary

(Dated: November 5, 2018)

Using the pre-LHC and LHC data for πp and pp diffractive collisions we study the ultrahigh energy asymptotic regime in the framework of the black disk picture. The black disk picture, being constrained by the s -channel unitarity condition and the t -channel analyticity, gives rather definite predictions for diffractive processes increasing with the energy. To deal with the data, we consider the Dakhno-Nikonov eikonal model which predicts a growth of the $\ln^2 s$ type for total and elastic cross sections and $(\tau = \mathbf{q}_\perp^2 \ln^2 s)$ -scaling for diffractive scattering and diffractive dissociation of hadrons. According to the calculations, ultrahigh energy asymptotic characteristics of diffractive and total cross sections are universal, and this results in the asymptotic equality of cross sections for all types of hadrons. We estimate the energy scale of the asymptotics in different processes. The manifestation of the asymptotic regime in hadron fragmentation reactions is discussed.

PACS numbers: 13.85.-t, 13.75.Cs, 14.20.Dh

I. INTRODUCTION

Experimental data for diffractive high energy collisions [1–3] definitely tell us that only at $\sqrt{s} \sim 7$ TeV we approach the energy region which can be called an asymptotic one. These are energies at which a picture of the black disk appears in the impact parameter space \mathbf{b} , see [4–6]. Actually, it is a black spot at $|\mathbf{b}| \simeq 0$; according to estimations only at $\sqrt{s} \sim 100$ TeV can one observe a shaped disk [6]. The problem we discuss here concerns possible predictions in the asymptotic energy region $\sqrt{s} \gtrsim 100$ TeV and the range of accuracy of the predictions.

The observed growth of total cross sections at pre-LHC energies [1] prompts investigations of models such as with a maximal increase allowed by the Froissart bound [7] or with power- s behaviour [8, 9]. Taking into account the s -channel unitarization of the scattering amplitude leads to damping of power- s growth to the $(\ln^2 s)$ -type, see [10–12]. Still, let us emphasize that exceeding the Froissart bound does not violate the general constraints for the scattering amplitude [13]. Presently the problem of unitarization of high energy amplitudes which correspond to increasing diffractive cross sections is a subject of intensive studies, see, for example, [14–17] and references therein.

A model for high-energy πp and $p^\pm p$ collisions was suggested by Dakhno and Nikonov [18] and successfully used for the description of the diffractive pre-LHC data, $\sqrt{s} \sim 0.2 - 1.8$ TeV. The model takes into account the quark structure of colliding hadrons, the gluon origin of the input pomeron and the colour screening effects in collisions. The model can be considered as a realization of

the Good-Walker eikonal approach [19] for a continuous set of channels.

In the paper [6] the diffractive pp -scattering was considered in terms of the Dakhno-Nikonov model, concentrating the attention on the ultra-high energy behaviour. The pp data were re-fitted taking into account new results in the TeV-region [2, 3]. The region 5-50 TeV turns out to be the one where the asymptotic behaviour starts; the asymptotic regime should reveal itself definitely at $10^2 - 10^4$ TeV.

For the ultra-high energy limit the Dakhno-Nikonov model predicts for total and elastic hadron-hadron cross sections a $(\ln^2 s)$ -growth: $\sigma_{tot} \sim \ln^2 s$, $\sigma_{el} \sim \ln^2 s$ and $[\sigma_{el}/\sigma_{tot}]_{\ln s \rightarrow \infty} \rightarrow 1/2$. The high energy cross sections $(\sigma_{el}, \sigma_{tot})$ approach their asymptotic values from bottom to top: $\sigma_{tot}(s)/\sigma_{tot}^{(asym)}(s) < 1$; this gives the illusion of exceeding the Froissart bound (see, for example, discussion in [20, 21]). Further, the model predicts that differential elastic cross sections depend asymptotically on transverse momenta with a relation for τ -scaling: $d\sigma_{el}(\tau)/d\tau = D(\tau)$ with $\int_0^\infty d\tau D(\tau) = \sigma_{el}(s)$ and $\tau = \mathbf{q}_\perp^2 \sigma_{tot} \propto \mathbf{q}_\perp^2 \ln^2 s$.

The model points to the universal behaviour of all total (and elastic) cross sections. It is the consequence of the universality of colliding disk structure (or the structure of parton clouds) at ultrahigh energy. But the question is at what energy range the asymptotic regimes are switched on for different processes; we have calculated here σ_{tot} , σ_{el} , σ_{inel} for pp , πp and $\pi\pi$ collisions.

Further, we consider diffractive dissociation processes. We demonstrate that these processes are increasing at asymptotic energies ($\sigma_D \propto \ln s$, $\sigma_{DD} \propto \ln s$) but their relative contribution tends to zero ($\sigma_D/\sigma_{tot} \rightarrow 0$,

$$\sigma_{DD}/\sigma_{tot} \rightarrow 0).$$

II. DIFFRACTIVE SCATTERING CROSS SECTIONS

The model is based on the hypothesis of gluonic origin of t -channel forces, and these gluons form pomerons. Hadrons, mesons (two-quark composite systems) and baryons (three-quark composite systems) scatter on the pomeron cloud. It is supposed that the pomeron cloud behaves as a low-density gas, and pomeron-pomeron interactions, as well as t -channel transitions of the type $P \rightarrow PP$, $P \rightarrow PPP$ and so on, can be neglected (for details see [18]).

The pomerons are formed by effective gluons (G) which are massive, $\sim 700 - 1000$ MeV [22, 23]. The pomeron parameter α'_P is small $\alpha'_P \simeq (0.10 - 0.25)$ GeV $^{-2}$, which means that pomerons are relatively heavy and hard [24]. The gluon structure of the pomeron provides colour screening effects for hadron quarks [25].

A. Formulae of the eikonal approach

Below we present formulae of the Dakhno-Nikonov model for the eikonal cross sections and then briefly discuss the used parametrization.

The total and elastic cross sections are:

$$\begin{aligned}\sigma_{tot}(AB) &= 2 \int d^2b \int dr' \varphi_A^2(r') dr'' \varphi_B^2(r'') \left[1 - \exp\left(-\frac{1}{2}\chi_{AB}(r', r'', \mathbf{b})\right) \right], \\ \sigma_{el}(AB) &= \int d^2b \left(\int dr' \varphi_A^2(r') dr'' \varphi_B^2(r'') \left[1 - \exp\left(-\frac{1}{2}\chi_{AB}(r', r'', \mathbf{b})\right) \right] \right)^2.\end{aligned}\quad (1)$$

Here $dr\varphi_A^2(r)$, $dr\varphi_B^2(r)$ are the quark densities of colliding hadrons:

$$\begin{aligned}dr\varphi_p^2(r) &= d^2r_1 d^2r_2 d^2r_3 \delta^{(2)}(\mathbf{r}_1 + \mathbf{r}_2 + \mathbf{r}_3) \varphi_p^2(r_1, r_2, r_3), \\ dr\varphi_\pi^2(r) &= d^2r_1 d^2r_2 \delta^{(2)}(\mathbf{r}_1 + \mathbf{r}_2) \varphi_\pi^2(r_1, r_2),\end{aligned}\quad (2)$$

where \mathbf{r}_a are the transverse coordinates of quarks, and φ_A^2 , φ_B^2 are given by quark wave functions squared integrated over longitudinal variables. Proton and pion quark densities are determined using the corresponding form factors; such an estimation can be found, for example, in [26].

The profile-function χ_{AB} describes the interaction of quarks via pomeron exchange as follows:

$$\begin{aligned}\chi_{AB}(r', r'', \mathbf{b}) &= \int d^2b' d^2b'' \delta^{(2)}(\mathbf{b} - \mathbf{b}' + \mathbf{b}'') \\ &\quad \times S_A(r', \mathbf{b}') S_B(r'', \mathbf{b}''), \\ S_\pi(r, \mathbf{b}) &= \rho(\mathbf{b} - \mathbf{r}_1) + \rho(\mathbf{b} - \mathbf{r}_2) \\ &\quad - 2\rho(\mathbf{b} - \frac{\mathbf{r}_1 + \mathbf{r}_2}{2}) \exp\left(-\frac{(\mathbf{r}_1 - \mathbf{r}_2)^2}{4r_{cs}^2}\right), \\ S_p(\mathbf{r}, \mathbf{b}) &= \sum_{i=1,2,3} \rho(\mathbf{b} - \mathbf{r}_i) \\ &\quad - \sum_{i \neq k} \rho(\mathbf{b} - \frac{\mathbf{r}_i + \mathbf{r}_k}{2}) \exp\left(-\frac{(\mathbf{r}_i - \mathbf{r}_k)^2}{4r_{cs}^2}\right).\end{aligned}\quad (3)$$

The term $\rho(\mathbf{b} - \mathbf{r}_i)$ describes the diagram where the pomeron is connected to one of the hadron quarks while the terms proportional to $\exp(-r_{ij}^2/r_{cs}^2)$ are related to the

diagram where the pomeron is connected to two quarks of the hadron. Such a diagram is a three-reggeon graph GGP where G is the reggeized gluon. Functions S_π and S_p tend to zero as $|\mathbf{r}_{ij}| \rightarrow 0$: this is the colour screening phenomenon inherent to the gluonic pomeron. For the sake of convenience one can perform calculations in the centre-of-mass system of the colliding quarks, supposing that the hadron momentum is shared equally between its quarks. Then

$$\begin{aligned}\rho(\mathbf{b}) &= \frac{g}{4\pi(G + \frac{1}{2}\alpha'_P \ln \frac{s}{s_0})} \exp\left[-\frac{\mathbf{b}^2}{4(G + \frac{1}{2}\alpha'_P \ln \frac{s}{s_0})}\right], \\ g^2 &= g_0^2 + g_1^2 \left(\frac{s_{qq}}{s_0}\right)^\Delta\end{aligned}\quad (4)$$

with the energy squared of the colliding quarks s_{qq} and $s_0 = 1$ GeV 2 . The parametrization of g^2 corresponds to the two-pole form of the QCD-motivated pomeron with intercepts $\alpha(0) = 1$ and $\alpha(0) = 1 + \Delta$.

As it was mentioned, the Dakhno-Nikonov model is actually a realization of the Good-Walker eikonal approach [19] for a continuous set of channels: each quark configuration with fixed coordinates is a separate channel. The two-pole pomeron exchange is popular from the sixties till now, see for example ref. [27].

B. Inelastic diffractive cross sections

The diffractive cross section for the two-particle reaction $A_1 B_1 \rightarrow A_2 B_2$ in the Dakhno-Nikonov eikonal ap-

proach reads:

$$\begin{aligned}
(2\pi)^2 \frac{d^2\sigma_{el}}{d^2q_\perp}(A_1 B_1 \rightarrow A_2 B_2) &= \int d^2b \, e^{i\mathbf{q}_\perp \mathbf{b}} \int d^2\tilde{b} \, e^{-i\mathbf{q}_\perp \tilde{\mathbf{b}}} \\
&\times \int dr' dr'' \varphi_{A_1}(r') \varphi_{B_1}(r'') \left[1 - \exp\left(-\frac{1}{2}\chi_{AB}(r', r'', \mathbf{b})\right) \right] \varphi_{A_2}(r') \varphi_{B_2}(r'') \\
&\times \int d\tilde{r}' d\tilde{r}'' \varphi_{A_1}(\tilde{r}') \varphi_{B_1}(\tilde{r}'') \left[1 - \exp\left(-\frac{1}{2}\chi_{AB}(\tilde{r}', \tilde{r}'', \tilde{\mathbf{b}})\right) \right] \varphi_{A_2}(\tilde{r}') \varphi_{B_2}(\tilde{r}''). \quad (5)
\end{aligned}$$

As a consequence of the universality of $\rho(\mathbf{r})$, the block $[1 - \exp(-\frac{1}{2}\chi_{AB}(r', r'', \mathbf{b}))]$ which is responsible for the interaction is universal and depends only on the type of colliding hadrons, mesons or baryons. This leads to the universal behaviour of cross sections at ultrahigh energies. The universality appears at energies when the essential values of $|\mathbf{b}|$ are much larger than the average interquark distances, $|\mathbf{b}| \gg \mathbf{r}$; in this region the integrations over impact parameters and interquark distances

are in fact separated.

A hadron in diffractive collision (to be definite, let it be A_1) can produce a set of similar states: these are transitions $A_1 \rightarrow A_1, A_2, A_3, \dots$. If the produced hadrons belong to a complete set of states, $\sum_n A_n \langle A_n^+ = I$, the sum of such processes gives a cross section $AB \rightarrow X_A + B$ which includes elastic and diffraction dissociation processes $X_A = A + X_{DA}$. This sum of cross sections is equal to:

$$\begin{aligned}
(2\pi)^2 \frac{d\sigma_{X(A)}}{d^2q_\perp}(AB \rightarrow X_A + B) &= \int d^2b \int d^2\tilde{b} \, e^{i\mathbf{q}_\perp \mathbf{b}} \, e^{-i\mathbf{q}_\perp \tilde{\mathbf{b}}} \int dr' dr'' d\tilde{r}'' \varphi_A^2(r') \varphi_B^2(r'') \varphi_B^2(\tilde{r}'') \\
&\times \left[1 - \exp\left(-\frac{1}{2}\chi_{AB}(r', r'', \mathbf{b})\right) \right] \left[1 - \exp\left(-\frac{1}{2}\chi_{AB}(r', \tilde{r}'', \tilde{\mathbf{b}})\right) \right]. \quad (6)
\end{aligned}$$

The cross section integrated over momenta transfer reads

$$\begin{aligned}
\sigma_{X(A)}(AB \rightarrow X_A + B) &= \int d^2b \int dr' dr'' d\tilde{r}'' \varphi_A^2(r') \varphi_B^2(r'') \varphi_B^2(\tilde{r}'') \\
&\times \left[1 - \exp\left(-\frac{1}{2}\chi_{AB}(r', r'', \mathbf{b})\right) \right] \left[1 - \exp\left(-\frac{1}{2}\chi_{AB}(r', \tilde{r}'', \mathbf{b})\right) \right]. \quad (7)
\end{aligned}$$

Let us recall that Eq. (7) gives us a sum of elastic and diffraction dissociation cross sections $\sigma_{X(A)}(AB \rightarrow X_A + B) = \sigma_{el}(AB) + \sigma_{D(A)}(AB)$. The sum of elastic and quasi-elastic cross sections $\sigma_{X(A)X(B)}(AB \rightarrow X_A + X_B)$ is determined by the relation:

$$\begin{aligned}
\sigma_{X(A)X(B)}(AB \rightarrow X_A + X_B) &= \sigma_{el}(AB) + \sigma_{D(A)}(AB) + \sigma_{D(B)}(AB) + \sigma_{D(A)D(B)}(AB) = \\
&= \int d^2b \int dr' dr'' \varphi_A^2(r') \varphi_B^2(r'') \left[1 - \exp\left(-\frac{1}{2}\chi_{AB}(r', r'', \mathbf{b})\right) \right]^2. \quad (8)
\end{aligned}$$

At $\ln s \rightarrow \infty$ this value tends to $\frac{1}{2}\sigma_{tot}$ from bottom to top [28]: $[\sigma_{el}(AB) + \sigma_{D(A)}(AB) + \sigma_{D(B)}(AB) + \sigma_{D(A)D(B)}(AB)]_{\ln s \rightarrow \infty} \rightarrow \frac{1}{2}\sigma_{tot}$, approaching the asymptotic regime for $\sigma_{X(A)X(B)}(AB \rightarrow X_A + X_B)$ is as quick as for $\sigma_{tot}(AB)$. Besides it means that at $\ln s \rightarrow \infty$ one has $[\sigma_{D(A)}(AB) + \sigma_{D(B)}(AB) + \sigma_{D(A)D(B)}(AB)]/\sigma_{tot}(DD) \rightarrow 0$.

But the experimental specification of the diffraction dissociation cross sections involved in Eq. (8) faces the problem of separation from events determined by the inner structure of the colliding disk, for example, that due to the three-pomeron diagram processes.

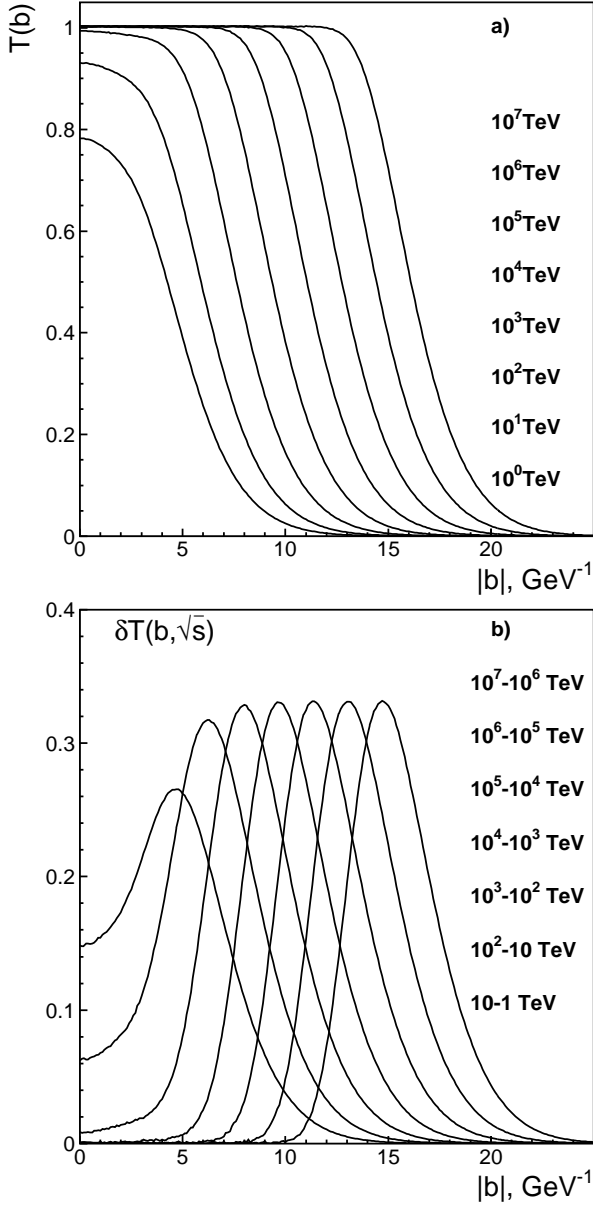


FIG. 1: a) Profile functions $T(b)$ determined in Eq. (10) at a set of energies $\sqrt{s} = 1, 10, 100, \dots, 10^7 \text{ TeV}$; b) The profile function growth factor determined as $\delta T(b, \sqrt{s}) = [T(b, 10\sqrt{s}) - T(b, \sqrt{s})]$ for $\sqrt{s} = 1, 10, 100, \dots, 10^6 \text{ TeV}$.

III. BLACK DISK PICTURE AND PREDICTIONS FOR THE ULTRAHIGH ENERGY REGION, $\sqrt{s} > 10^2 \text{ TEV}$

The predictions we give are definitely related to the picture of the black disk. The freedom of predictions is connected to the rate of the black disk radius growth and the detailed structure of the black disk boundary. Just to fix this freedom we use the Dakhno-Nikonov model considering it as reasonably realistic. The parameters

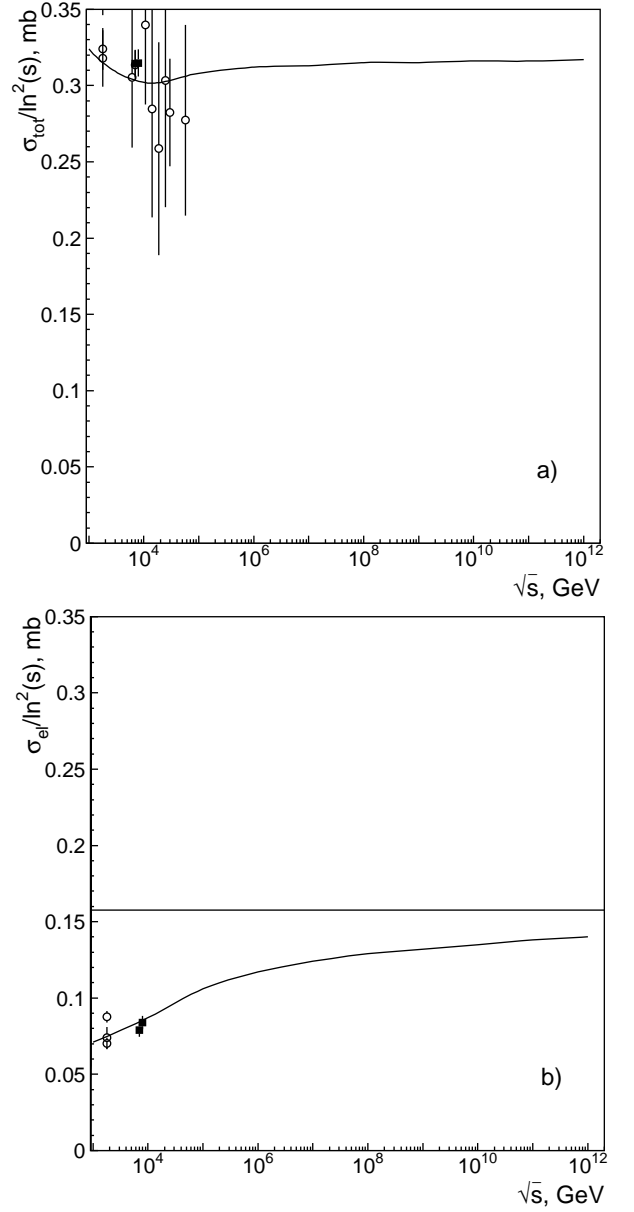


FIG. 2: Total and elastic cross section data [1–3] versus fit curves for (a) $\sigma_{tot}(pp)/\ln^2 s$ and (b) $\sigma_{el}(pp)/\ln^2 s$, where \sqrt{s} in GeV units, in the Dakhno-Nikonov model for the energy region $\sqrt{s} > 1 \text{ TeV}$. The straight line is the asymptotic limit for the elastic cross section: $\sigma_{el}(s) = \sigma_{tot}^{(asym)}/2$.

are

parameters	ref. [6]
Δ	0.273
$g_0^2 [\text{mb}]$	8.106
$g_1^2 [\text{mb}/\text{GeV}^2\Delta]$	0.379
$\alpha_P' [(\text{GeV}/c)^{-2}]$	0.129
$G [(\text{GeV}/c)^{-2}]$	-0.365
$r_{cs}^2 [(\text{GeV}/c)^{-2}]$	0.670

(9)

The profile function $T(b)$, calculated using the parameters of Eq. (9), predicts the black disk regime at

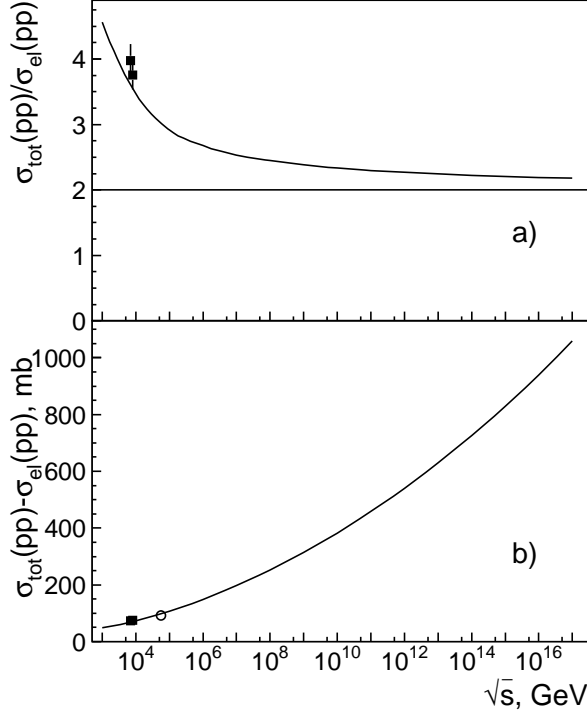


FIG. 3: Proton-proton collisions: a) the ratio $\sigma_{tot}(pp)/\sigma_{el}(pp) \rightarrow 2$ and b) its difference, $\sigma_{inel}(pp) = \sigma_{tot}(pp) - \sigma_{el}(pp) \propto \ln^2 s$; data from refs. [2, 3].

$\sqrt{s} \gtrsim 10^2$ TeV. The profile function is determined as follows:

$$\begin{aligned} \sigma_{tot} &= 2 \int d^2b T(b) = 2 \int d^2b \left[1 - e^{-\frac{1}{2}\chi(b)} \right], \\ 4\pi \frac{d\sigma_{el}}{d\mathbf{q}_\perp^2} &= A^2(\mathbf{q}_\perp^2), \\ A(\mathbf{q}_\perp) &= \int d^2b e^{i\mathbf{b}\mathbf{q}_\perp} T(b). \end{aligned} \quad (10)$$

This is shown in Fig. 1a for pre-LHC, LHC and ultrahigh energies. The profile functions $T(b)$ are not saturated at $\sqrt{s} \sim 0.5 - 2.0$ TeV being $T(b) < 1$. According to the fit, a black spot ($T(b) \simeq 1$ at $b < 2\text{GeV}^{-1} \simeq 0.4\text{fm}$) appears at $\sqrt{s} \sim 50 - 100$ TeV; this phenomenon indicates the start of the black disk regime. At $\ln s \gg 1$, when the asymptotic regime works, there are two clear regions in the b -space (Fig. 1a): with $T(b) \simeq 1$ (black disk area) and $T(b) \simeq 0$ (transparent area). Conventionally we determine these areas by the constraints

$$\begin{aligned} b^2 &< 4\Delta\alpha'_P \ln^2 \frac{s}{s_-}, \quad \text{with } T(b) > 0.97, \\ b^2 &> 4\Delta\alpha'_P \ln^2 \frac{s}{s_+}, \quad \text{with } T(b) < 0.03, \end{aligned} \quad (11)$$

giving the black disk radius:

$$R_{black} = 2\sqrt{\Delta\alpha'_P} \ln \frac{s}{s_R}, \quad \sqrt{s_R} \simeq 80 \text{ GeV}. \quad (12)$$

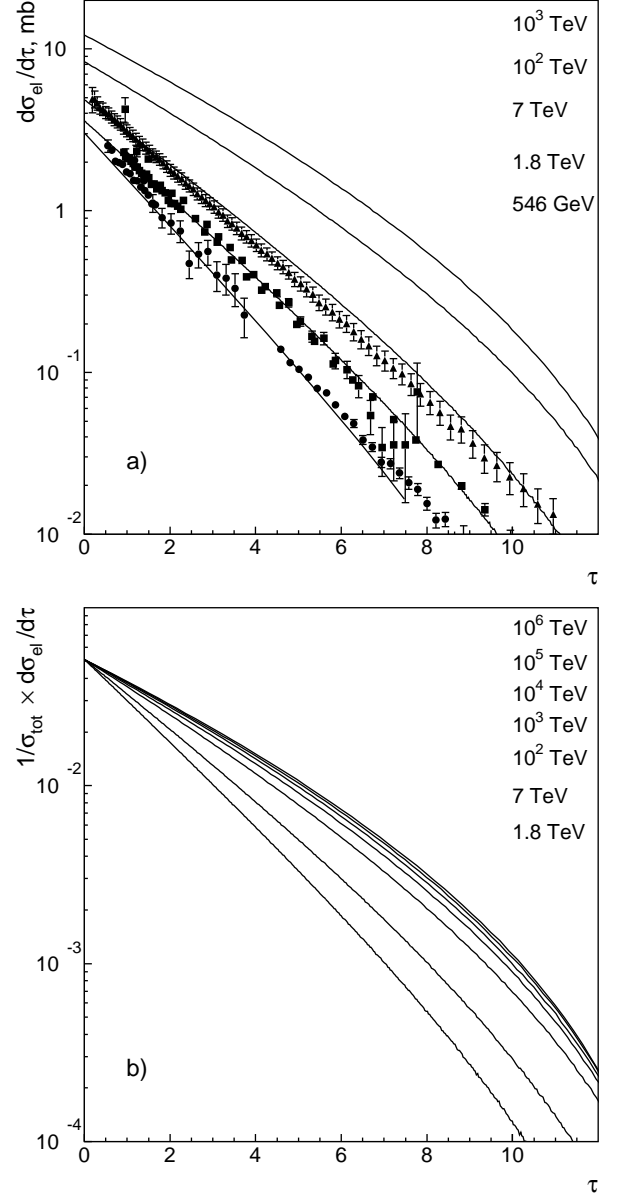


FIG. 4: a) Differential cross sections $d\sigma_{el}/d\tau$, where $\tau = \sigma_{tot}\mathbf{q}_\perp^2$, at $\sqrt{s} = 0.546, 1.8, 7.0$ TeV and their descriptions in the Dakhno-Nikonov model; b) Calculated differential cross sections $1/\sigma_{tot} \times d\sigma_{el}/d\tau$ at $\sqrt{s} = 1, 10, 100, 1000, \dots, 10^6$ TeV and their approach to the τ -scaling limit.

The black disk radius depends on parameters of the leading pomeron only, (factor $\sqrt{\Delta\alpha'_P}$), which results in Gribov's universality of hadronic total cross sections at asymptotic energies [29].

The growth of the profile function, $\delta T(b, \sqrt{s}) \equiv [T(b, 10\sqrt{s}) - T(b, \sqrt{s})]$, is demonstrated in Fig. 1b. Steady values of areas under $\delta T(b, \sqrt{s})$ tell us that the ratio of contributions of the border region to that of the internal disk region is decreasing with energy $\sigma_{inel}^{border}/\sigma_{inel}^{intern} \rightarrow 1/\ln s$. It is revealed as a basis for the black disk description of asymptotic cross sections.

In Fig. 2 we show total and elastic cross sections in the $\sqrt{s} \sim 1 - 100$ TeV region [1–3] and their description in the fit of ref. [6]. An extension of the fitting curves into the $\sqrt{s} > 100$ TeV region tells us that we have a relatively fast approach to the asymptotic behaviour for $\sigma_{tot}/\ln^2 s$; the approach of $\sigma_{el}/\ln^2 s$ to the asymptotic value is slow. A slow switching on of asymptotics is definitely seen in the ratio $\sigma_{tot}(pp)/\sigma_{el}(pp)$, Fig. 3a. The inelastic cross section $\sigma_{inel}(pp) = \sigma_{tot}(pp) - \sigma_{el}(pp) \propto \ln^2 s$ is demonstrated in Fig. 3b.

In Fig. 4a we show $d\sigma_{el}/d\tau$ (let us recall that $\tau = \sigma_{tot} \mathbf{q}_\perp^2$) at ISR and LHC energies; the approach of $1/\sigma_{tot} \times d\sigma_{el}/d\tau$ to the τ -scaling limit is demonstrated in Fig. 4b.

In Fig. 5a we show the ratio

$$\frac{\sigma_{X(p)X(p)}(pp) - \sigma_{el}(pp)}{\sigma_{tot}(pp)} = \frac{2\sigma_{D(p)}(pp) + \sigma_{D(p)D(p)}(pp)}{\sigma_{tot}(pp)}, \quad (13)$$

see Eq. (8). It tends to zero at $\ln s \rightarrow \infty$, this fact is in complete agreement with $\sigma_{tot}/\sigma_{el} \rightarrow 2$. In Fig. 5b we show the sum $2\sigma_{D(p)}(pp) + \sigma_{D(p)D(p)}(pp)$, it increases as

$$\sigma_{X(p)X(p)}(pp) - \sigma_{el}(pp) \simeq 0.58 \ln \frac{s}{s_{el}^{XX}} \text{ mb}, \quad s_{el}^{XX} \simeq 1.22 \text{ GeV}^2. \quad (14)$$

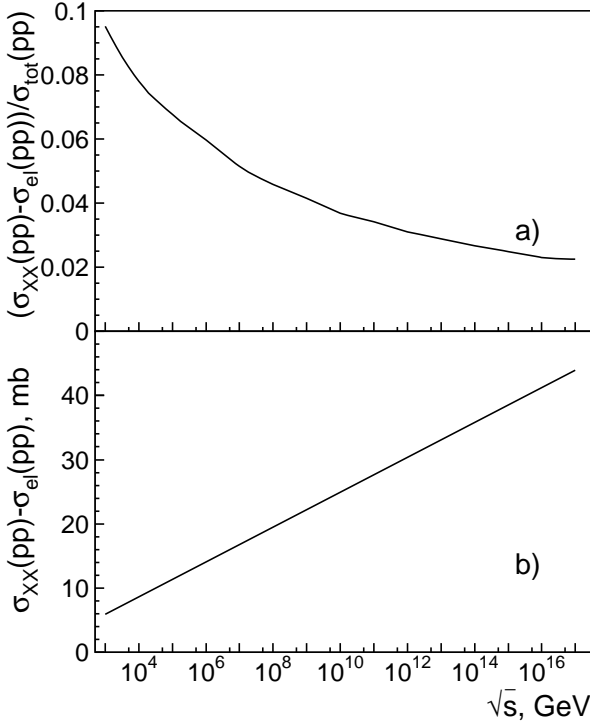


FIG. 5: a) The ratio given in Eq. (13) and b) the difference $\sigma_{X(p)X(p)}(pp) - \sigma_{el}(pp) = 2\sigma_{D(p)}(pp) + \sigma_{D(p)D(p)}(pp) \propto \ln s$.

The ratio $Re A_{el}/Im A_{el}$ at $\mathbf{q}_\perp^2 \simeq 0$ at asymptotic energies is determined by the analyticity of the scattering

amplitude:

$$A_{el} \propto i[\ln^2(s/s_0) + \ln^2(-s/s_0)], \quad \frac{Re A_{el}}{Im A_{el}} \simeq \frac{\pi}{\ln(s/s_0)} \quad (15)$$

This estimation gives us $Re A_{el}/Im A_{el} = 0.18 \pm 0.04$ for the $\sqrt{s} \gtrsim 100$ TeV region, being in qualitative agreement with the 7-TeV data: $Re A_{el}/Im A_{el} = 0.14^{+0.01}_{-0.08}$ [2].

The extension of the results on πp collisions does not cause problems in the Dakhno-Nikonov model since for that the addition of the pion quark distribution is needed only. The distribution of quarks in a pion is known (see, for example, ref. [26]) and this allows to give predictions.

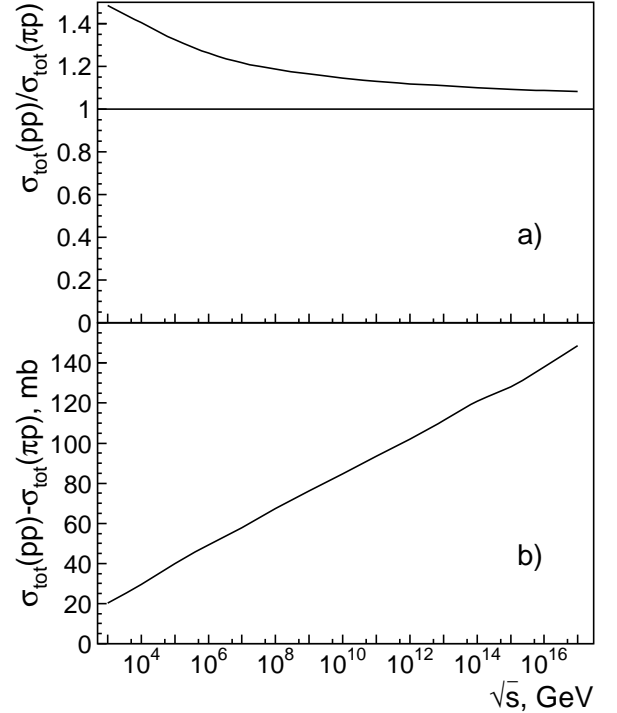


FIG. 6: a) Ratio of proton-proton and pion-proton total cross sections, $\sigma_{tot}(pp)/\sigma_{tot}(\pi p) \rightarrow 1$, and b) its difference $\sigma_{tot}(pp) - \sigma_{tot}(\pi p) \propto \ln s$.

The ratio $\sigma_{tot}(pp)/\sigma_{tot}(\pi p)$ is shown in Fig. 6a; it asymptotically tends to 1. The difference of proton-proton and pion-proton total cross sections increases with energy and can be described at $\sqrt{s} \gtrsim 10^6$ GeV as

$$\sigma_{tot}(pp) - \sigma_{tot}(\pi p) \simeq 1.91 \ln \frac{s}{s_{\pi p}^{pp}} \text{ mb}, \quad s_{\pi p}^{pp} \simeq 6.25 \text{ GeV}^2. \quad (16)$$

The universality of the total cross sections means the equality of the leading terms ($\propto \ln^2 s$) only, and it is demonstrated in Fig. 7a where $\sigma_{tot}(pp)$, $\sigma_{tot}(\pi p)$ and $\sigma_{tot}(\pi\pi)$ are shown. For comparison we show the approach to the asymptotic limit of diffractive cross sections in pp collisions, Fig. 7b: the Miettinen-Pumplin limit value $\frac{1}{2}\sigma_{tot}(pp)$, elastic plus single diffraction dissociation processes $\sigma_{el}(pp) + 2\sigma_{D(p)}(pp)$ and $\sigma_{el}(pp)$. Here we def-

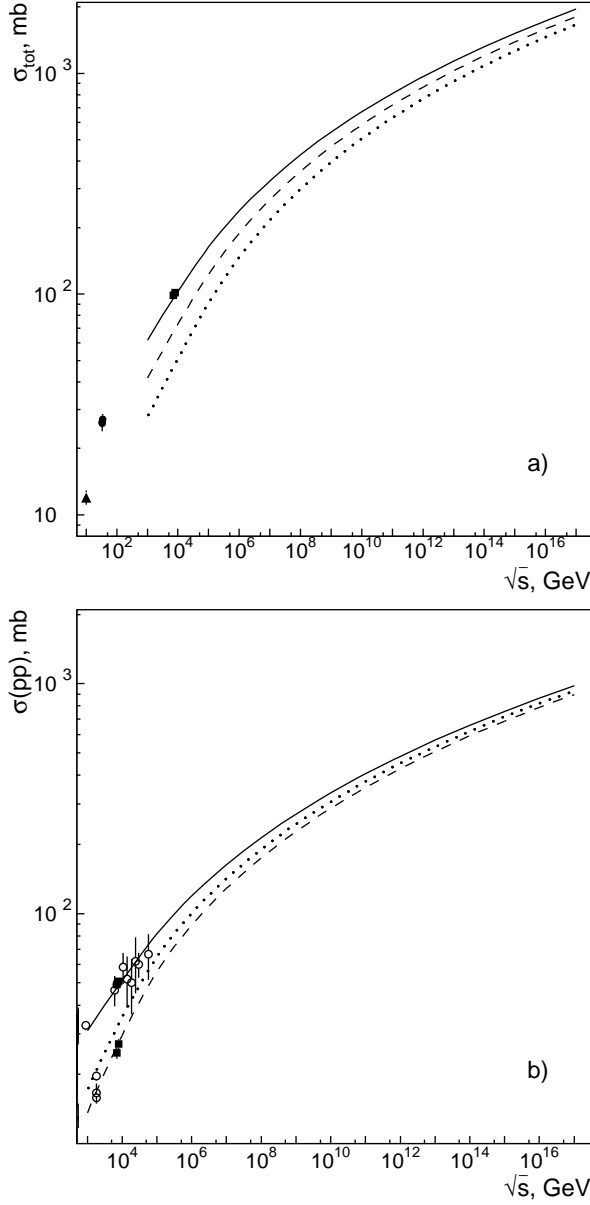


FIG. 7: a) Total cross sections: $\sigma_{tot}(pp)$ (solid line), $\sigma_{tot}(\pi\pi)$ (dashed line) and $\sigma_{tot}(\pi\pi)$ (dotted line). Squares (pp) are from [2], circles ($\pi\pi$) are from [30], triangles ($\pi\pi$) are from [31]. b) Proton-proton collisions: $\frac{1}{2}\sigma_{tot}(pp)$ (solid line), $\sigma_{el}(pp) + 2\sigma_{D(p)}(pp)$ (dotted line) and $\sigma_{el}(pp)$ (dashed line). Data [1–3] stand for $\frac{1}{2}\sigma_{tot}(pp)$ and $\sigma_{el}(pp)$.

initely see a more rapid switching on of the asymptotic regime.

We perform the unitarization of the scattering amplitude supposing it originates from conventional pomerons, though other types of input pomerons are possible as well as non-pomeron short-range contributions (for example, see [32–35]). But here we concentrate our attention on peripheral interactions and their transformation with energy growth. Small deviations of the fitting curves from data can be easily improved using some kind of short-

range contributions.

IV. CONCLUSION

In ref. [6] the description of diffractive pp collisions was performed in terms of the Dakhno-Nikonov model for pre-LHC and LHC energies: with parameters found in [6] we study here the ultrahigh energy region where the asymptotic regime works.

The twofold structure of hadrons – hadrons are built from constituent quarks; the latter are formed by clouds of partons which manifest itself in high energy hadron collisions. At moderately high energies colliding protons reveal themselves in impact parameter space as three disks corresponding to three constituent quarks. At ultrahigh energies the situation is transformed to a one-disk picture, and the energy of this transformation is that of LHC. The radius of the black disk at asymptotic energies increases as $\ln s$, hence providing a $\ln^2 s$ growth of σ_{tot} , σ_{el} with $\sigma_{el}/\sigma_{tot} \rightarrow 1/2$ and a τ -scaling for diffractive cross sections.

The calculations we have carried out demonstrate a comparatively fast approach of $\sigma_{tot}(s)$ to asymptotic behaviour (Fig. 2a), in contrast to $\sigma_{el}(s)$ (Fig. 2b). It also means a slow approach of $\sigma_{inel}(s) = \sigma_{tot}(s) - \sigma_{el}(s)$ to the asymptotic behaviour.

A good level of description of the diffractive pp scattering is demonstrated on Fig. 4. It is seen that the τ -scaling for $1/\sigma_{tot} \times d\sigma_{el}/d\tau$ is at work within 10% accuracy at $\sqrt{s} \gtrsim 100$ TeV (the upper curves in Fig. 4b).

The change of the regime, from the constituent quark collision picture to that with a united single disk, was discussed [36–38] when definite indications about hadron cross section growth appeared. It is emphasized that the single black disk regime should change probabilities of productions of hadrons in the fragmentation region (hadrons with $x = p/p_{in} \sim 1$); for a more detailed discussion of the scaling violation in the hadron fragmentation region see [39].

Diffractive dissociation processes are increasing at asymptotic energies. For pp collisions the relative weights of quasi-elastic cross sections are vanishing with the energy growth, $\sigma_{D(p)}(pp \rightarrow pX)/\sigma_{tot}(pp) \rightarrow 0$ and $\sigma_{D(p)D(p)}(pp \rightarrow XX)/\sigma_{tot}(pp) \rightarrow 0$, while the cross sections increases, $2\sigma_{D(p)}(pp \rightarrow pX) + \sigma_{D(p)D(p)}(pp \rightarrow XX) \simeq 0.58 \ln s/s_{el}^{XX}$ mb. It means we can estimate diffractive production cross section of $N_{\frac{1}{2}}(1440)$ as $(\frac{1}{2} \div \frac{1}{10}) 0.58 \ln s/s_{el}^{XX}$ mb.

A steady increase of the black disk radius $R_{black} \propto \sqrt{\Delta \alpha'_P \ln s}$, is determined by parameters of the leading t -channel singularity: the pomeron intercept $\alpha(0) = 1 + \Delta$ ($\Delta > 0$) and the pomeron trajectory slope α'_P . The s -channel unitarization of the scattering amplitude damps the strong pomeron pole singularity, transforming it into a multipomeron one. Therefore, we face an intersection of problems of the gluon content of t -channel states at ultrahigh energies and the physics of gluonic states, glueballs.

At present the glueball states are subjects of discussions, see, for example [40–42] and references therein. Studies of phenomenons related to glueballs and multigluon states at small $|t|$ (or, at small masses) are enlightening for the confinement singularity - see discussion in ref. [43]. The large value of mass of the soft effective gluon (and the corresponding value the low-lying glueballs) and the slow rate of the black disk increase appear to be related phenomena.

V. ACKNOWLEDGMENT

We thank Ya.I. Azimov, D.V. Bugg, A.K. Likhoded, M.G. Ryskin, and A.V. Sarantsev for useful discussions and comments. The work was supported by grants RFBR-13-02-00425 and RSGSS-4801.2012.2 .

-
- [1] UA4 Collaboration, Phys. Lett. **B147** , 385 (1984); UA4/2 Collaboration, Phys. Lett. **B316**, 448 (1993); UA1 Collaboration, Phys. Lett. **B128**, 336 (1982); E710 Collaboration, Phys. Lett. **B247**, 127 (1990); CDF Collaboration, Phys. Rev. **D50**, 5518 (1994).
 - [2] G. Latino for the TOTEM collaboration, *Summary of Physics Results from the TOTEM Experiment*, arXiv:1302.2098(2013) [hep-ph].
 - [3] Pierre Auger Collaboration (P. Abreu et al.), Phys. Rev. Lett. **109**, 062002 (2012).
 - [4] M.M. Block and F. Halzen, Phys. Rev D **86**, 051504 (2012).
 - [5] M.G. Ryskin, A.D. Martin and V.A. Khoze, Eur. Phys. J. C **72**, 1937 (2012).
 - [6] V.V. Anisovich, K.V. Nikonov and V.A. Nikonov, Phys. Rev D **88**, 014039 (2013); arXiv:1306.1735v2 [hep-ph].
 - [7] M. Froissart, Phys. Rev. **123**, 1053 (1961).
 - [8] A.B. Kaidalov and K.A. Ter-Martirosyan, Sov. J. Nucl. Phys. **39**, 979 (1984).
 - [9] A. Donnachie and P.V. Landshoff, Nucl. Phys. **B231**, 189 (1984).
 - [10] T.K. Gaisser and T. Stanev, Phys. Lett., **B219**, 375, 1989.
 - [11] M. Block, F. Halzen and B. Margolis, Phys. Lett., **B252**, 481, 1990.
 - [12] R.S. Fletcher, Phys. Rev. **D46**, 187 (1992).
 - [13] Y.I. Azimov, Phys. Rev. **D84**, 056012 (2011); arXiv:1208.4304(2012) [hep-ph].
 - [14] F. Halzen, K. Igi, M. Ishida and C.S. Kim, arXiv:1110.1479V2(2012) [hep-ph].
 - [15] V. Uzhinsky and A. Galoyan, arXiv:1111.4984v5(2012) [hep-ph].
 - [16] V.A. Schegelsky, M.G. Ryskin, Phys. Rev. **D85**, 094024 (2012).
 - [17] E. Martynov, Phys. Rev. **D87**, 114018 (2013).
 - [18] L.G. Dakhno and V.A. Nikonov, Eur. Phys. J. A **8**, 209 (1999).
 - [19] M.L. Good, W.D. Walker, Phys. Rev. **120**, 1857 (1960).
 - [20] M.M. Block and F. Halzen, arXiv:1210.4086v1 (2012) [hep-ph].
 - [21] M.J. Menon and P.V.R.G. Silva, arXiv:1212.5096v1(2012) [hep-ph].
 - [22] G. Parisi and R. Petronzio, Phys. Lett. **B94**, 51 (1980).
 - [23] M. Consoli, J.H. Field, Phys. Rev. **D49**, 1293 (1994).
 - [24] V.N. Gribov, Nucl. Phys. **B106**, 189 (1976).
 - [25] V.V. Anisovich, L.G. Dakhno, and V.A. Nikonov, Phys. Rev. **D44**, 1385 (1991).
 - [26] V.V. Anisovich, D.I. Melikhov, and V.A. Nikonov, Phys. Rev. **D52**, 5295 (1995).
 - [27] A. Donnachie and P.V. Landshoff, arXiv:1112.2485, (2011) [hep-ph]; arXiv:1309.1292, (2013) [hep-ph]
 - [28] H.I. Miettinen and J. Pumplin Phys. Rev. **D18**, 1696 (1978).
 - [29] V.N. Gribov, Yad. Fiz. **17**, 603 (1973), [Sov. J. Nucl. Phys. **17**, 313 (1973)].
 - [30] U. Dersch *et al.* [SELEX Collaboration], Nucl. Phys. B **579**, 277 (2000) [hep-ex/9910052].
 - [31] H. Abramowicz, M. Gorski, G. Sinapius, A. Wroblewski, A. Zieminski, H. J. Lubatti, K. Moriyasu and C. D. Rees *et al.*, Nucl. Phys. B **166**, 62 (1980).
 - [32] A.V. Kotikov and L.N. Lipatov, Nucl. Phys. **B661**, 19 (2003).
 - [33] K. Kang and H. Nastase, Phys. Lett. **B624**, 125 (2005).
 - [34] E. Gotsman, E.M. Levin and U. Maor, arXiv:1203.2419 (2012).
 - [35] A.K. Likhoded, A.V. Luchinsky and A.A. Novoselov, Phys. Rev. **D82**, 114006 (2010).
 - [36] V.V. Anisovich and V.M. Shekhter, Yad. Fiz. **28**, 1079 (1978), [Sov. J. Nucl. Phys. **28**, 554 (1978)].
 - [37] V.V. Anisovich, E.M. Levin and M.G. Ryskin, Yad. Fiz. **29**, 1311 (1979), [Sov. J. Nucl. Phys. **29**, 674 (1979)].
 - [38] V.V. Anisovich, V.M. Braun and Yu.M. Shabelski, Yad. Fiz. **36**, 1556 (1982), [Sov. J. Nucl. Phys. **36**, 904 (1982)].
 - [39] V.V. Anisovich, M.N. Kobrinsky, J. Nyiri, Yu.M. Shabelski, *Quark model and high energy collisions*, Second Edition, World Scientific, Singapore (2004).
 - [40] V.V. Anisovich, Usp. Fiz. Nauk **47** (2004) 45 [Phys. Usp. **47** (2004) 45].
 - [41] E. Klempt and A. Zaitsev, Phys. Rept. **454** (2007) 1.
 - [42] W. Ochs, J. Phys. **40** (2013) 043001.
 - [43] A.V. Anisovich, V.A. Nikonov, A.V. Sarantsev, V.V. Anisovich, M.A. Matveev, T.O. Vulfs, K.V. Nikonov, J. Nyiri, Phys. Rev. **D84** 076001 (2011).